Supplemental Material

Electrogenerated Chemiluminescence of $Ru(bpy)_3^{2+}$/Arginine System: A Specific and Sensitive Detection of Acetaminophen

Yi Xiao[1,4], Guofang Wang[1], Haomin Yi[1], Suhua Chen[3], Qinyu Wu[1], Siyi Zhang[1], Kexin Deng[1], Simeng Zhang[1], Zi-Qi Shi[2*], Xiaoping Yang[1*]

1. Key Laboratory of Study and Discovery of Small Targeted Molecules of Hunan Province, Department of Pharmacy, School of Medicine, Hunan Normal University, Changsha 410013, Hunan, China

2. Affiliated Hospital of Integrated Traditional Chinese and Western Medicine, Nanjing University of Chinese Medicine, Nanjing 210028, Jiangsu, China

3. Hunan Provincial Maternal and Child Health Care Hospital, Changsha 410008, Hunan, China

4. John A. Paulson School of Engineering and Applied Sciences, Harvard University, Cambridge, MA 02138, USA.

*Corresponding authors. Email address: Xiaoping.Yang@hunnu.edu.cn; shiziqi47@126.com.

Table of Content

S1. Morphology of MPS

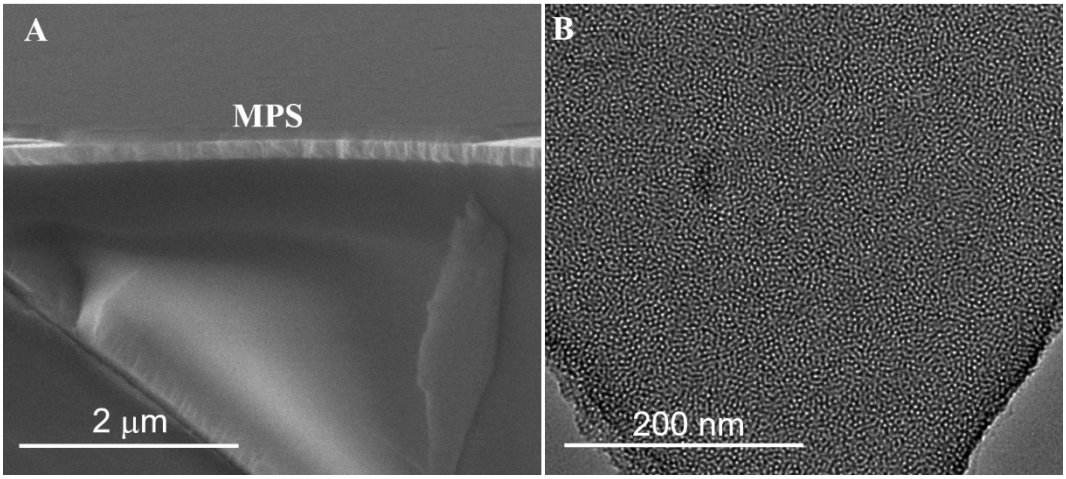

Fig. S1. Morphology of MPS. (A) SEM image shows that MPS is above the indium tin oxide glass. (B) TEM image shows MPS is vertically aligned nanochannels (indicated as white pores).

S2. CVs of $Ru(bpy)_3^{2+}$/Arg system

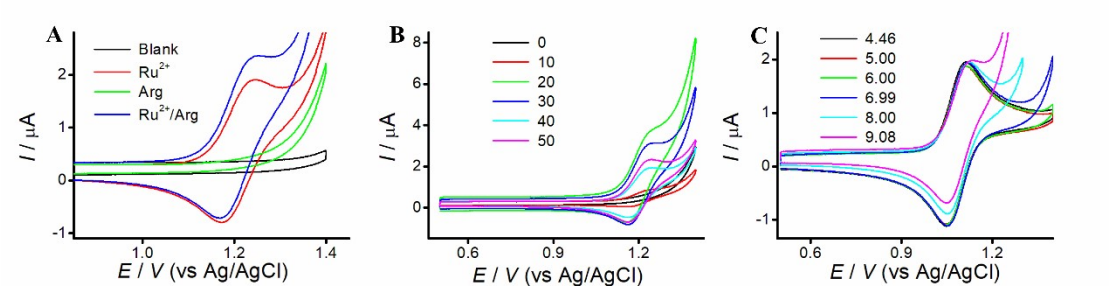

Fig. S2 CVs of $Ru(bpy)_3^{2+}$/Arg system. A. CVs of 50 μM $Ru(bpy)_3^{2+}$ and 50 μM Arg. B. CVs of different concentrations of $Ru(bpy)_3^{2+}$ with 50 μM Arg. C. CVs of different pH with 50 μM $Ru(bpy)_3^{2+}$ and 50 μM Arg. Scan rate: 0.05 V s^{-1}.

S3. Mechanism of $Ru(bpy)_3^{2+}$/TPrA system

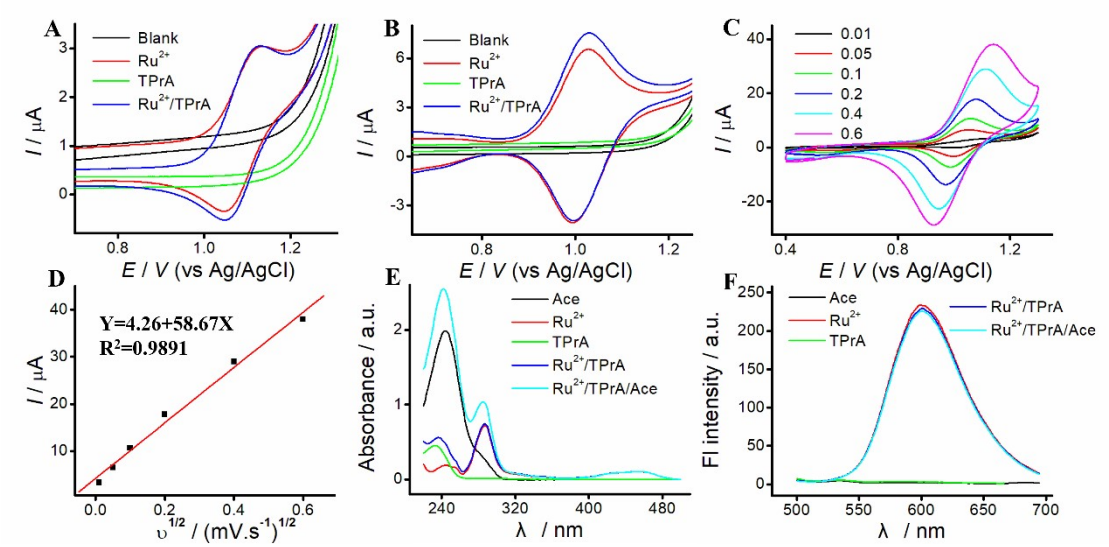

Fig. S3 Mechanism of $Ru(bpy)_3^{2+}$/TPrA system. A. CVs of different solutions at ITO electrode. Scan rate: 0.05 V s^{-1}. B. CVs of different solutions at MPS electrode. C. CVs of different scan rates with 50 μM $Ru(bpy)_3^{2+}$ and 50 μM TPrA at ITO electrode. D. Linear plot of oxidation peak current intensity *vs.* $v^{1/2}$. E. UV–vis absorption of different solutions. F. Fluorescence spectra of different solutions (λ_{exc} = 452 nm).

S4. CVs of $Ru(bpy)_3^{2+}$/DBAE system

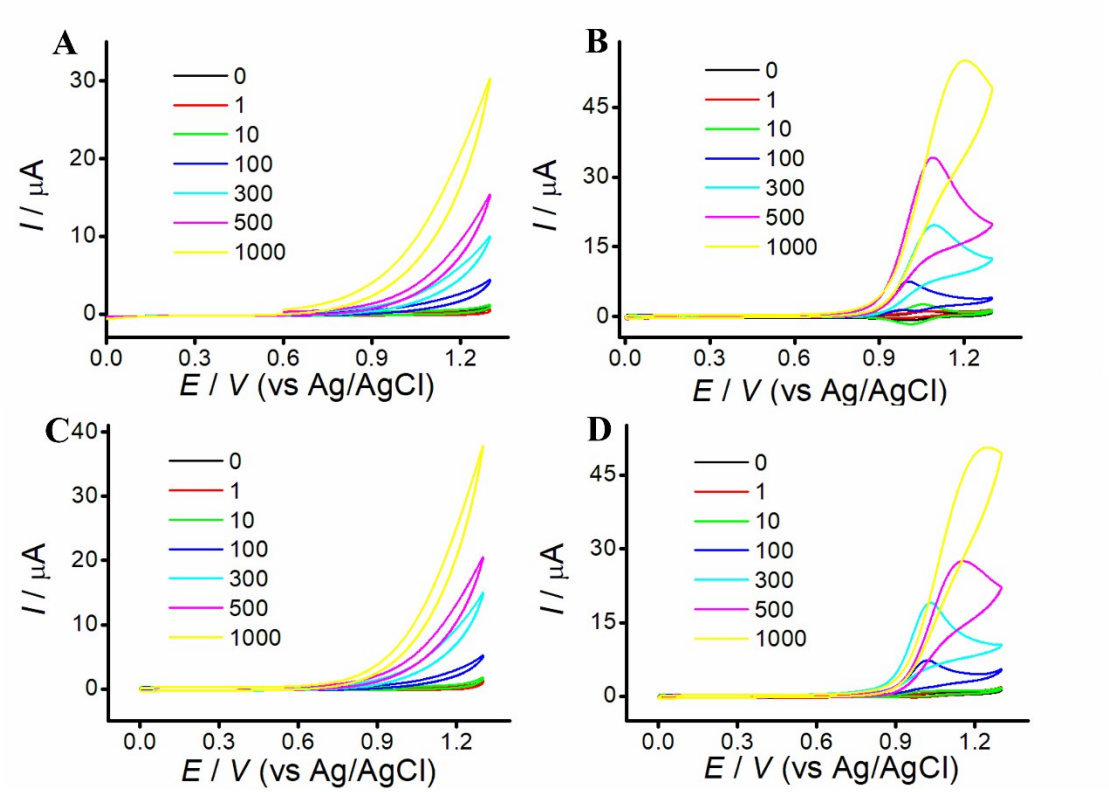

Fig. S4 CVs of $Ru(bpy)_3^{2+}$/DBAE system. A. CVs of different concentration of Ace (0.1 M PBS, pH 9.21) at MPS electrode with scan rate of 0.05 V/s. B. CVs of different concentration of Ace with 50 μM $Ru(bpy)_3^{2+}$ at MPS electrode. C. CVs of different concentration of Ace with 50 μM DBAE at MPS electrode. D. CVs of different concentration of Ace with 50 μM $Ru(bpy)_3^{2+}$ and 50 μM DBAE at MPS electrode.

S5. Mechanism of $Ru(bpy)_3^{2+}$/DBAE system

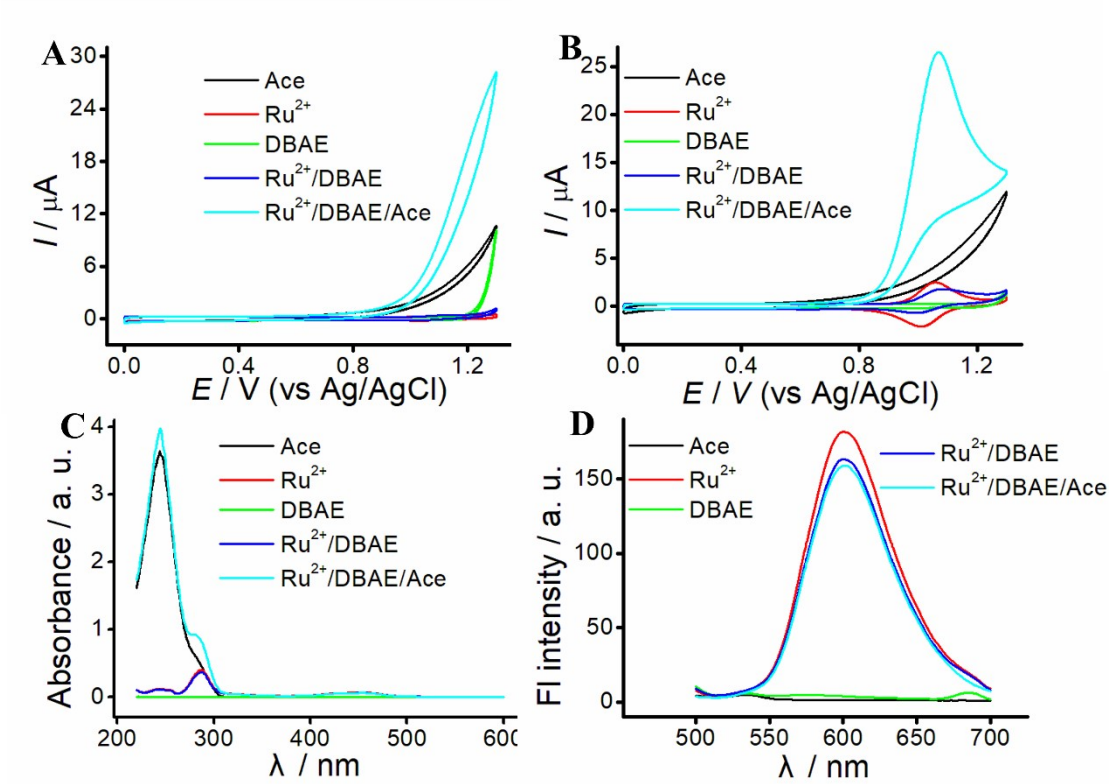

Fig. S5 Mechanism of $Ru(bpy)_3^{2+}$/DBAE system. A. CVs of different solutions at ITO electrode with scan rate of 0.05 V/s. B. CVs of different solutions at MPS electrode. C. UV–vis absorption of different solutions. D. Fluorescence spectra of different solutions (λ_{exc} = 452 nm).

S6. Specificity of MPS-ECL sensor

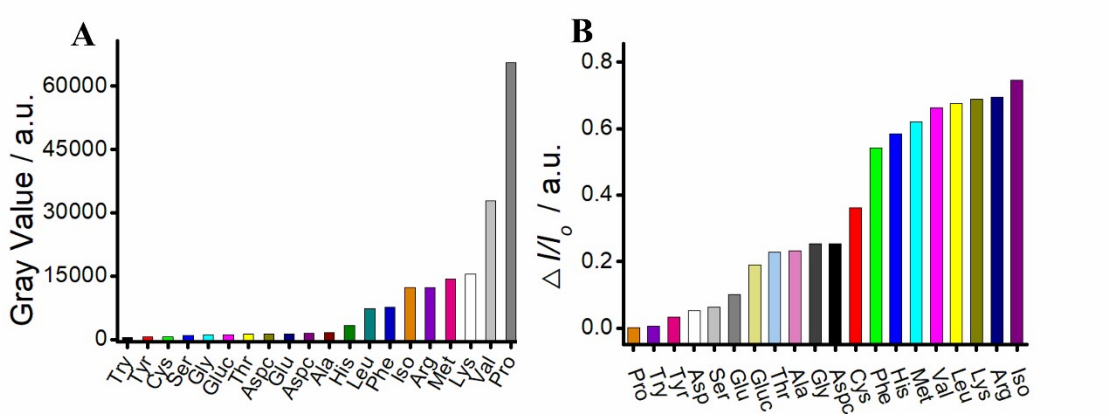

Fig. S6. Specificity of the MPS-ECL sensor. (A) ECL intensity of 20 types of amino acids on MPS-ECL sensor in PBS containing $Ru(bpy)_3^{2+}$. (B) ECL quenching effect of 20 types of amino acids on MPS-ECL sensor in $Ru(bpy)_3^{2+}$/Ace system.

S7. Repeatability and temperature stability of ECL system

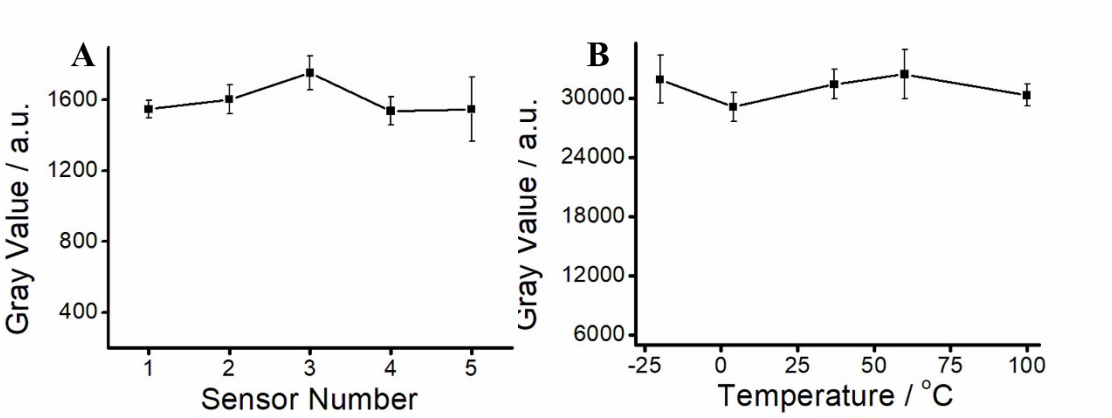

Fig. S7 A. Repeatability of ECL system. B. Temperature stability of ECL system.

Table S1. Analytical results for different co-reactants on MPS-ECL sensor

Table S1. Analytical results for different co-reactants on MPS-ECL sensor

Different co-reatants	Fitting equation	Dynamic range (μM)	LOD (μM)	R^2
Arg	Y=88.55X+4653.91	1–700	0.590	0.9974
TPrA	Y=1811.79X+4564.30	0.1–30	0.023	0.9839
DBAE	Y=3169.74X+3652.29	0.5–20	0.027	0.9928

Table S2. Analytical results for Ace by different ECL systems

Table S2. Analytical results for Ace by different ECL systems

Different ECL systems	Fitting equation	LOD (μM)	Dynamic range (μM)	R^2
$Ru(bpy)_3^{2+}$/Arg	Y=0.00202X-0.00907	0.84	1–500	0.9828
$Ru(bpy)_3^{2+}$/TPrA	Y=0.0018X-0.5225	8.08	10–500	0.9877
$Ru(bpy)_3^{2+}$/DBAE	Y=0.00176X-0.4190	5.98	10–500	0.9611

Table S3. Analytical results for Arg by MPS-ECL sensor in biological fluids

Table S3. Analytical results for Arg by MPS-ECL sensor in biological fluids

Biological fluids	Added (μM)	Found (μM)	Recovery (%)	RSD (%)
Human serum	500	467.500	93.50	0.58
Human saliva	300	283.350	94.45	3.59

Table S4. Analytical results for Ace by MPS-ECL sensor in biological fluids

Table S4. Analytical results for Ace by MPS-ECL sensor in biological fluids

Biological fluids	Added (μM)	Found (μM)	Recovery (%)	RSD (%)
Human serum	150	163.832	109.22	1.89
Human saliva	50	50.750	101.5	2.60

Table S5. Analytical results for Ace by HPLC in biological fluids

Table S5. Analytical results for Ace by HPLC in biological fluids

Fitting equation	Fitting equation	Dynamic range (μM)	LOD (μM)	LOQ (μM)	R^2
Human serum	Y=41.355X-9.8885	16–1649	0.097	0.195	0.9996
Human saliva			0.039	0.0474	

Table S6. Ace contents in biological fluids by HPLC and MPS-ECL sensor

Table S6. Ace contents in biological fluids by HPLC and MPS-ECL sensor

Biological fluids	MPS-ECL sensor		HPLC	
	Concentration (μM)	RSD (%)	Concentration (μM)	RSD (%)
Human serum	54.933	2.09	48.740	0.169
Human saliva	50.750	2.60	47.368	0.563